Contrib Mineral Petrol (1993) 113:9–23

Contributions to Mineralogy and Petrology

Isotope and trace element evidence for three component mixing in the genesis of the North Luzon arc lavas (Philippines)

F. McDermott[1], M.J. Defant[2], C.J. Hawkesworth[1], R.C. Maury[3], and J.L. Joron[4]

[1] Department of Earth Sciences, The Open University, Walton Hall, Milton Keynes, MK7 6AA, UK
[2] Department of Geology, University of South Florida, Tampa, FL 33620-5200, USA
[3] Département des Sciences de la Terre, Université de Bretagne Occidentale, Faculté des Sciences, Avenue Le Gorgeu, F-29283 Brest, France
[4] Groupe des Sciences de la Terre, C.E.N. Sacley, F-91191 Gif-sur-Yvette, France

Received March 11, 1992/Accepted July 6, 1992

Abstract. Post-3Ma volcanics from the N Luzon arc exhibit systematic variations in $^{87}Sr/^{86}Sr$ (0.70327–0.70610), $^{143}Nd/^{144}Nd$ (0.51302–0.51229) and $^{208}Pb^{*}/^{206}Pb^{*}$ (0.981–1.035) along the arc over a distance of about 500 km. Sediments from the South China Sea west of the Manila Trench also exhibit striking latitudinal variations in radiogenic isotope ratios, and much of the isotopic range in the volcanics is attributed to variations in the sediment added to the mantle wedge during subduction. However, Pb-Pb isotope plots reveal that prior to subduction, the mantle end-member had high $\Delta 8/4$, and to a lesser extent high $\Delta 7/4$, similar to that in MORB from the Indian Ocean and the Philippine Sea Plate. Th isotope data on selected Holocene lavas indicate a source with unusually high Th/U ratios (4.5 – 5.5). Combined trace element and isotope data require that three end-members were implicated in the genesis of the N Luzon lavas: (1) a mantle wedge end-member with a Dupal-type Pb isotope signature, (2) a high LIL/HFS 'subduction component' interpreted to be a slab-derived hydrous fluid, and (3) an isotopically enriched end-member which reflects bulk addition ($<5\%$) of subducted S China Sea terrigenous sediment. The $^{87}Sr/^{86}Sr$ ratios in the volcanics show a restricted range compared with that in the sediments, and this contrasts with $^{143}Nd/^{144}Nd$ and $^{208}Pb^{*}/^{206}Pb^{*}$, both of which have similar ranges in the volcanics and sediments. Such differences imply that whereas the isotope ratios of Nd, Pb and Th are dominated by the component from subducted sediment, those of Sr reflect a larger relative contribution from the slab-derived fluid.

Introduction

Many subduction-related rocks exhibit a distinctive trace element signature, namely high large ion lithophile (LIL) and low high field strength (HFS) element contents relative to N-type MORB (e.g. Hawkesworth et al. 1979; Kay 1980; Pearce 1983). The source of the 'excess' LIL elements remains controversial, and in part it reflects contributions from altered oceanic crust (e.g. De Paolo and Wasserburg 1977; Hawkesworth et al. 1977, 1979), subducted sediment (e.g. Kay et al. 1978; Kay 1980; Sun 1980) and the mantle wedge (Arculus 1981; Morris and Hart 1983; Gill 1984; Hawkesworth and Ellam 1989). The extent to which the subducted slab and the mantle wedge contribute to the LIL element inventory of subduction-related rocks is important for models of destructive-plate margin magmatism, crustal recycling and crustal growth in this tectonic setting. Also at issue is whether the HFS element depletions reflect the presence of residual HFS element-rich mineral phases in the subducted slab (Saunders et al. 1980), in the mantle wedge (Green 1980; Morris and Hart 1983), or simply reflect the relative mobilities of LIL and HFS elements in slab-derived hydrous fluids (e.g. Tatsumi et al. 1986, McCulloch and Gamble 1991).

High LIL/HFS ratios are often accompanied by light rare earth element (LREE) enrichment, and in a recent review, Hawkesworth et al. (1991) considered destructive plate-margin rocks in two groups, characterized by low and high Ce/Yb ratios. The two groups not only have different trace element ratios (e.g. Rb/Sr, Sm/Nd, Th/U), but they also have different Sr, Nd and Pb isotope characteristics which indicate that the trace element fractionations are relatively old, and pre-date subduction by several 100 Ma (Hawkesworth et al. 1991; McDermott and Hawkesworth 1991). Rocks with low (<15) Ce/Yb (for example from the Marianas, Tonga, and the Aleutians) tend to have relatively low $^{87}Sr/^{86}Sr$, high $^{143}Nd/^{144}Nd$ and high ($^{230}Th/^{232}Th$), with average values of 0.7033, 0.51302 and 1.1, respectively. It has been argued that these isotope ratios preclude large fluxes of slab-derived LREEs, Sr, Pb or Th, and if correct this interpretation implies that a significant proportion of these elements are derived from the mantle wedge (e.g. Morris and Hart 1983; Hawkesworth et al. 1991). By contrast, rocks in the high (>15) Ce/Yb group (e.g. the Aeolian Islands, N Philippines) exhibit wide ranges in Sr, Nd, Pb and Th isotope ratios. These 'enriched' isotope signatures require a contribution from material which is both old and relatively enriched in incompatible elements

Correspondence to: F. McDermott

(high Rb/Sr, low Sm/Nd, etc.), and in principle such material could reflect subducted sediment, old trace element enriched mantle in the mantle wedge and/or contamination by the arc crust. We demonstrate that in the case of the N Luzon volcanics the effects of crustal contamination are minimal, and then attempt to evaluate critically the roles of sediment subduction and old trace element enriched mantle in the generation of the enriched trace element and isotope characteristics of the N Luzon (Philippines) rocks, a suite which appears to be typical of many high Ce/Yb subduction-related lavas.

Geological setting

The N Luzon volcanic arc comprises a chain of stratovolcanoes which extend for about 1200 km in an approximately north-south direction from Mindoro (13°N), to the east coast of Taiwan (23°N). The northern 500 km of this arc, from Baguio (16°N) to Lutao (23°N), is the subject of this study (Fig. 1), and in this region the arc has been sub-divided into three segments; the North Luzon, Babuyan and Taiwan segments (Defant et al. 1989, 1990). Volcanism appears to have occurred in two episodes, the earliest of which commenced during the late Eocene and continued until the middle Miocene. This early phase of volcanism was associated with subduction of the Indian Ocean Plate beneath the western rim of the Philippine Plate, and the products of this volcanism have been described by Knittel et al. (1988) and Mukasa et al. (1987). Magmatism appears to have ceased in the late Oligocene, but at about 15 Ma subduction resumed and construction of the present-day N Luzon arc commenced. The post-15 Ma volcanism is associated with subduction along the Manila Trench of the South China Sea oceanic basin which opened in the period 32–17 Ma (Taylor and Hayes 1983). The Manila Trench is > 5 km deep west of Luzon and it contains 1–2km of turbidites transported along the trench from Taiwan and the Chinese continental margin (Hayes and Lewis 1984). Geochemical models for the evolution of the N Luzon volcanics must therefore take account of: (1) early Miocene subduction of Indian Ocean MORB and possibly Indian Ocean pelagic sediments, (2) The young (< 50 Ma) age of the oceanic lithosphere and the probable absence of old arc-crust or old lithospheric mantle in the region of the present-day N Luzon arc, and (3) that the South China Sea basin opened close to the edge of the Chinese continental margin (Rangin et al. 1990), so that most of the sediments subducted in the north of the arc since 15 Ma are likely to have been terrigenous rather than pelagic in origin.

Mt. Cagua volcano in the southern part of the N Luzon arc is built upon late Oligocene basaltic lava flows, and the exposed basement in the central portion of the arc consists of recent volcanics with no evidence for a sialic basement. The N Luzon lavas are predominantly andesites with minor basalts and rhyolites, and their K-Ar ages range from 30 Ma to < 1 Ma (Richard et al. 1986; Lan et al. 1986; Bellon et al. 1988). The rocks range from tholeiitic to high-K calc-alkaline (< 0.2 2.6% K_2O), and display a distinct increase in K_2O with time (Richard et al. 1986; Jacques 1987; Defant et al. 1990).

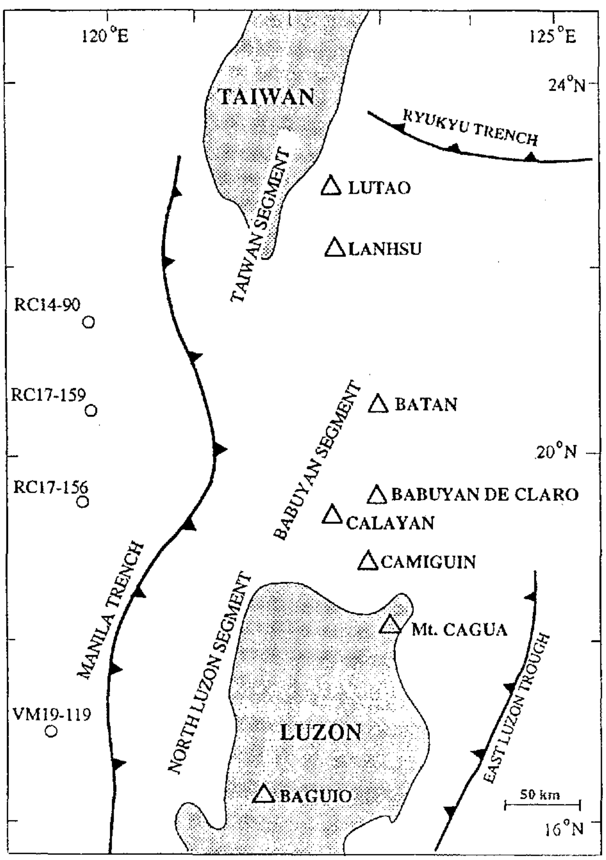

Fig. 1. Map showing the distribution of the major volcanic centres (*triangles*) in the N Luzon arc from Luzon to Taiwan. Active subduction occurs along the Manila Trench. Also shown are the S. China Sea sediment core sites

Samples studied and analytical techniques

The rocks selected for analyses are basalts, basaltic andesites and andesites from seven strato-volcanoes at Baguio, Mt. Cagua, Camiguin, Babuyan de Claro, Batan, Lanhsu and Lutao (Fig. 1). With the exception of two samples from Lanhsu (TW 31 and TW 32) which are 3.9 and 5.5 Ma, respectively (Defant et al. 1990), the samples selected for isotope work are all younger than 3 Ma in order to minimize the effects of possible temporal changes in lava chemistry. The Batan samples are predominantly high-K calc-alkaline basalts and basaltic andesites, whereas those from Mt. Cagua, Babuyan de Claro, and Lanhsu are calc-alkaline basalts, basaltic andesites and andesites (Fig. 2a). New Pb isotope analyses are presented for 35 samples, and new Sr and Nd isotope determinations have been undertaken on 20 of these to go with the previously published data by Defant et al. (1990). The results of both studies are listed in Table 1. The new Sr and Nd isotope data either plot within or extend slightly the published data fields. The samples selected for Th isotope measurements are from historic or ^{14}C dated young (< 2000 years) lava flows from Babuyan de Claro and Batan (Fig. 1). In addition, Pb, Sr and Nd isotope ratios of selected sediments from the China Sea were analyzed to constrain better the isotope composition of sedimentary material being subducted along the Manila Trench (Table 1). In the absence of suitable DSDP core material, piston cores of South China Sea sediment (Fig. 1) were sampled at the Lamont Doherty core facility. The cores were sampled at 50 m intervals, and 0.3 g aliquots from each sample were combined, mixed, and crushed for analysis. The outer surface of the core was discarded and the upper 10 cm of each core was not sampled to avoid the possibility of anthropogenic contamination.

Sr and Nd isotope ratios were analyzed in peak-switching mode on a Finnigan MAT 261 mass-spectrometer. NBS 987 gave a mean value of 0.710235 $\pm$ 20, and the Johnson and Mattey Nd standard gave a value of 0.511842 $\pm$ 16 (2 standard deviations on the mean of 10 analyses). Pb was analyzed in static mode in temperature controlled runs (1150°C), and the ratios were corrected for a 0.1% a.m.u.$^{-1}$ fractionation relative to the recommended values for NBS 981 (Catanzaro 1968). Replicate analyses (Table 1) indicate that the external precision of the Pb isotope results is better than 0.08%. Th and U contents were analyzed by isotope dilution using a ^{229}Th - ^{235}U tracer and are reproducible to $\pm$ 1%. Th/U atomic ratios

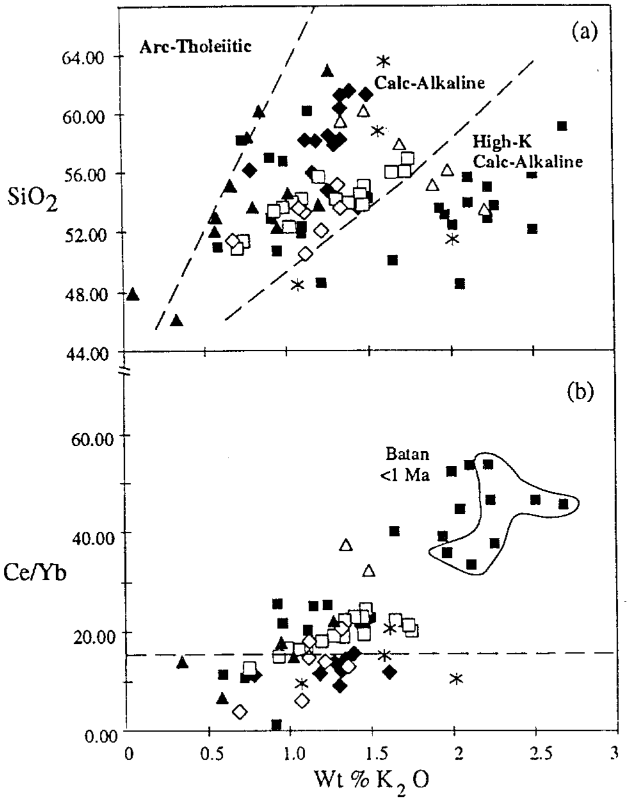

Fig. 2a. SiO_2 vs. K_2O variation diagram for the post-3Ma N Luzon lavas. Fields are from Peccerrilo and Taylor 1976. *Filled diamonds*, Camiguin Island; *asterisks*, Baguio; *open diamonds*, Mt. Cagua; *filled triangles*, Lanhsu; *open squares*, Babuyan de Claro; *filled squares*, Batan; *open triangles*, Lutao. **b** Ce/Yb versus K_2O diagram showing that high Ce/Yb ratios are associated with high K contents, and that many of the K-rich samples from Batan are < 1 Ma old. Symbols as in Fig. a

were converted to weight ratios, and these are expressed as activity ratios, hereafter denoted by parentheses, using the relationship Th/U (weight ratio) $= 3.034/(^{238}U/^{232}Th)$, (Condomines et al. 1988). Th isotope ratios were analyzed in static mode on a Finnigan MAT 261 mass-spectrometer equipped with a secondary electron multiplier, pulse conditioning circuitry, and a Hewlett Packard 5316B ion-counter to measure the minor (^{230}Th) peak. The abundance sensitivity of this mass-spectrometer measured at two mass units from a major peak is approximately 1 ppm, so that 10–20% of the ^{230}Th peak represents a contribution from the much larger (1–5 pA) ^{232}Th peak. This background contribution is subtracted by measuring the count-rate at masses 229.7 and 230.7, before and several times during each sample run, and by interpolating between the measured count-rates at 229.7 and 230.7 using an empirically determined background curve. Mass spectrometric Th isotope determinations yield the atomic ratio of $^{230}Th/^{232}Th$, but to facilitate comparison with published Th isotope data, we have converted the measured atomic ratios to activity ratios, using decay constants of $4.948 \times 10^{-11}\ a^{-1}$ and $9.217 \times 10^{-6}\ a^{-1}$ for ^{232}Th and ^{230}Th, respectively (Le Roux and Glendenin 1963; Meadows et al. 1980). Within-run precision based on counting statistics is typically 0.5–1.0%, depending on the ($^{230}Th/^{232}Th$) ratio of the sample and the intensity of the ^{232}Th ion-beam, and the run-to-run precision is $\pm$ 1.5% (2σ). Three measurements of an Iceland glass standard (A-THO) yielded ($^{230}Th/^{232}Th$) ratios of 1.018 $\pm$ 9, 1.020 $\pm$ 5 and 1.021 $\pm$ 7 respectively, all of which are indistinguishable from the alpha-spectrometric value of 1.028 $\pm$ 14 (M. Condomines, personal communication 1990). The accuracy of the measured $^{230}Th/^{232}Th$ ratios was checked by measuring several samples analyzed previously by alpha-spectrometry, and was independently verified by analyzing Th, U and ($^{230}Th/^{232}Th$) in several old ($>$ 300 ka), international rock standards which define an equiline on a ($^{230}Th/^{232}Th$) versus ($^{238}U/^{232}Th$) diagram (McDermott et al. in press).

Major and trace element data

The N Luzon lavas are basalts, basaltic andesites and andesites, many of which are relatively K-rich. In detail, all samples younger than 1 Ma from the island of Batan plot in the high-K calc-alkaline field (Fig. 2a) whereas most of the older samples ($>$ 2Ma) plot in the calc-alkaline field, reflecting the previously documented increase in K_2O with time in many of the N Luzon volcanic centres (Defant et al. 1990). This shift with time to higher K_2O is accompanied by a change in isotope ratios, with $^{87}Sr/^{86}Sr$, for example, increasing from $<$ 0.7040 in pre-1 Ma Batan lavas to $>$ 0.7044 in the Recent lavas (see later). The two Lanhsu samples are relatively old ($>$ 3.9 Ma), and these have the lowest K_2O for a given SiO_2 content. K_2O clearly increases with SiO_2 in some suites (e.g. Babuyan de Claro) although such intra-suite differentiation is unlikely to be responsible for the wide range in K_2O at a given SiO_2 content.

The lavas have the relatively high LIL element contents characteristic of destructive-plate margin rocks, and typically they also have relatively high LREE abundances. The degree of LREE enrichment, as indicated by the Ce/Yb ratio shows a broad positive correlation with K_2O (Fig. 2b). A striking feature of the lavas is their wide range in incompatible trace element abundances. A previous study (Defant et al. 1990) showed that the REE profiles vary from relatively flat patterns (x10 chondrite) in Calayan, to strongly LREE enriched (x500 chondrite) in samples from Lutao. Th abundances vary from $<$ 3 ppm in Mt. Cagua to $>$ 30 ppm in the high-K calc-alkaline suite from Batan, and two LREE-enriched samples from Lutao have approximately 80 ppm Th (Table 2). Ta abundances vary by at least an order of magnitude, from 0.1 ppm in Babuyan de Claro to 1.0 ppm in the LREE enriched Lutao samples (Table 2). Sm/Nd ratios decrease northwards from Mt. Cagua to Batan, but increase north of Batan through Lanhsu to Lutao (Fig. 3c). Rb/Sr and Rb/Ba ratios mirror the variations in Sm/Nd and are highest near the centre of the arc in Batan and Babuyan de Claro where Sm/Nd is low (Fig. 3a, b).

Radiogenic isotopes

Sr and Nd isotopes

$^{87}Sr/^{86}Sr$ ratios range from 0.70327 on Camiguin Island to 0.70610 on Lutao, and $^{143}Nd/^{144}Nd$ varies from 0.51229 on Lutao to 0.51296 on Baguio (Table 1). Many of the samples plot below the 'mantle array' on a Nd-Sr isotope diagram (Fig. 4), consistent with the published isotope results for the N Luzon volcanics (Defant et al. 1989, 1990) and ultramafic xenoliths from Batan (Vidal et al. 1989). In detail, the combination of isotope and trace

Table 1. Sr, Nd, Pb and Th isotope data for the N. Luzon are volcanics

Sample	Rock type	Age	$^{87}Sr/^{86}Sr$	$^{143}Nd/^{144}Nd$	$^{206}Pb/^{204}Pb$	$^{207}Pb/^{204}Pb$	$^{208}Pb/^{204}Pb$
Batan Island							
B 3M	B. Andesite	1480 ± 50a	0.70476	0.51248	18.426	15.589	38.662
					(18.425)	(15.605)	(38.700)
B 10	B. Andesite	2310 ± 80a	0.70445	0.51255	18.298	15.538	38.492
B 1E	B. Andesite	< 0.10 Ma	0.70479	0.51250	18.400	15.581	38.632
B 5	B. Andesite	0.01 Ma		0.51262	18.411	15.612	38.691
B 7	B. Andesite	1480 ± 50a	0.70435	0.51255	18.373	15.590	38.597
B 82	B. Andesite	0.45 ± 0.13	0.70459	0.51254	18.370	15.581	38.604
B 88	B. Andesite	0.76 ± 0.04	0.70545	0.51239	18.378	15.594	38.661
B 93	Basalt	1.07 ± 0.16	0.70393	0.51264	18.373	15.581	38.599
B 42	Andesite	1.09 ± 0.08	0.70393	0.51251	18.360	15.558	38.516
B 46	B. Andesite	2.32 Ma	0.70359	0.51272	18.388	15.588	38.585
B 83	Basalt		0.70481		18.411	15.604	38.694
B 86	Basalt	1.71 Ma	0.70380	0.51273			
B 80	Basalt	2.96 Ma	0.70396	0.51255			
Babuyan de Claro							
Bb 1	B. Andesite		0.70434	0.51265	18.516	15.625	38.790
Bb 2	B. Andesite	0.01 Ma	0.70466	0.51263	18.519	15.621	38.796
Bb 17	Andesite	0.90 Ma	0.70448	0.51259			
Bb 20	Andesite	1.68 Ma	0.70457	0.51256	18.531	15.614	38.837
Bb 21	B. Andesite	0.80 Ma	0.70448	0.51263	18.504	15.608	38.747
Bb 22	B. Andesite	0.01 Ma	0.70467	0.51256	18.523	15.614	38.765
					(18.542)	(15.631)	(38.820)
Bb 27	B. Andesite	0.83 Ma	0.70449	0.51261	18.510	15.610	38.755
Bb 3	B. Andesite	1.05 Ma	0.70455	0.51262	18.529	15.629	38.812
Bb 39	Basalt	1.14 Ma	0.70448	0.51258	18.515	15.621	38.782
Camiguin Island							
Cm 12	Andesite	0.40 ± 0.12 Ma	0.70356	0.51299	18.398	15.547	38.466
Cm 5	Andesite	0.69 ± 0.10 Ma	0.70327	0.51302	18.370	15.543	38.425
Cm 51	Andesite	1.52 Ma	0.70407	0.51281			
Cm 54	B. Andesite	0.74 ± 0.06 Ma	0.70404	0.51278	18.500	15.609	38.731
Cm 33	Andesite	< 0.40 Ma	0.70358	0.51292	18.367	15.562	38.440
Cm 35	Andesite	0.86 ± 0.26 Ma	0.70355	0.51293	18.382	15.560	38.490
Cm 19	Andesite	1.01 ± 0.15 Ma	0.70380	0.51278	18.425	15.566	38.555
Mt Cagua							
Ca 2	Basalt	1.27 Ma	0.70386	0.51286	18.575	15.609	38.775
Ca 11	Basalt	0.32 ± 0.05 Ma	0.70388		18.492	15.530	38.590
Ca 9	B. Andesite	0.64 ± 0.19 Ma	0.70386	0.51264	18.502	15.574	38.645
Ca 26	B. Andesite	< 10, 000 a	0.70395	0.51287	18.569	15.615	38.804
Lanhsu							
TW 31	B. Andesite	3.90 Ma	0.70431	0.51274	18.298	15.573	38.561
TW 32	B. Andesite	5.45 Ma	0.70545	0.51264	18.394	15.622	38.781
Lutao							
TW 36	Basaltic Andesite	1.90 Ma	0.70610	0.51229	18.424	15.639	38.845
TW 40	Andesite	2.90 Ma	0.70601	0.51231	18.429	15.637	38.830
TW 41	Andesite		0.70483	0.51259	18.412	15.611	38.698
Baguio							
47 A	Basalt	2.90 Ma	0.70377	0.51294	18.348	15.532	38.343
38 A	Basalt	2.80 Ma	0.70379	0.51295			
PL 41	Andesite	0.80 Ma	0.70388	0.51295			
PL 72	Andesite		0.70366	0.51296			

element data (see also Fig. 11) suggest that two trends may be recognized. Thus, many of the samples from the southern segment of the arc, notably those from Baguio, Camiguin and Mt. Cagua, plot close to or within the mantle array (trend A, Fig. 4 inset). This contrasts with those from Babuyan de Claro, Batan and Lutao to the north of the arc (Fig. 1) all of which define a trend displaced below, but sub-parallel to the mantle array (trend B, Fig. 4 inset).

It is noticeable that the Batan samples define two trends on Fig. 4. The older Batan lavas (> 1Ma) exhibit a restricted range in $^{87}Sr/^{86}Sr$ (0.70359–0.70396) and they define a steep array on Fig. 4, whereas the younger Batan lavas display a wider range in $^{87}Sr/^{86}Sr$

Table 1 (continued)

$^{208}Pb^*/^{206}Pb^*$	$(^{230}Th/^{232}Th)$	$(^{238}U/^{232}Th)$
1.007	0.553 ± 3	0.550 ± 5
1.010		
1.003	0.560 ± 3	0.550 ± 5
1.007	0.552 ± 3	0.583 ± 6
1.012		
1.006		
1.007		
1.013		
1.006		
0.999		
1.003		
1.013		
1.011		
1.018	0.669 ± 7	0.703 ± 7
1.015		
1.008		
1.008		
1.008		
1.012		
1.010		
0.989		
0.988		
1.007		
0.989		
0.993		
0.996		
1.003		
0.992		
0.997		
1.007		
1.010		
1.024		
1.028		
1.035		
1.013		
0.981		

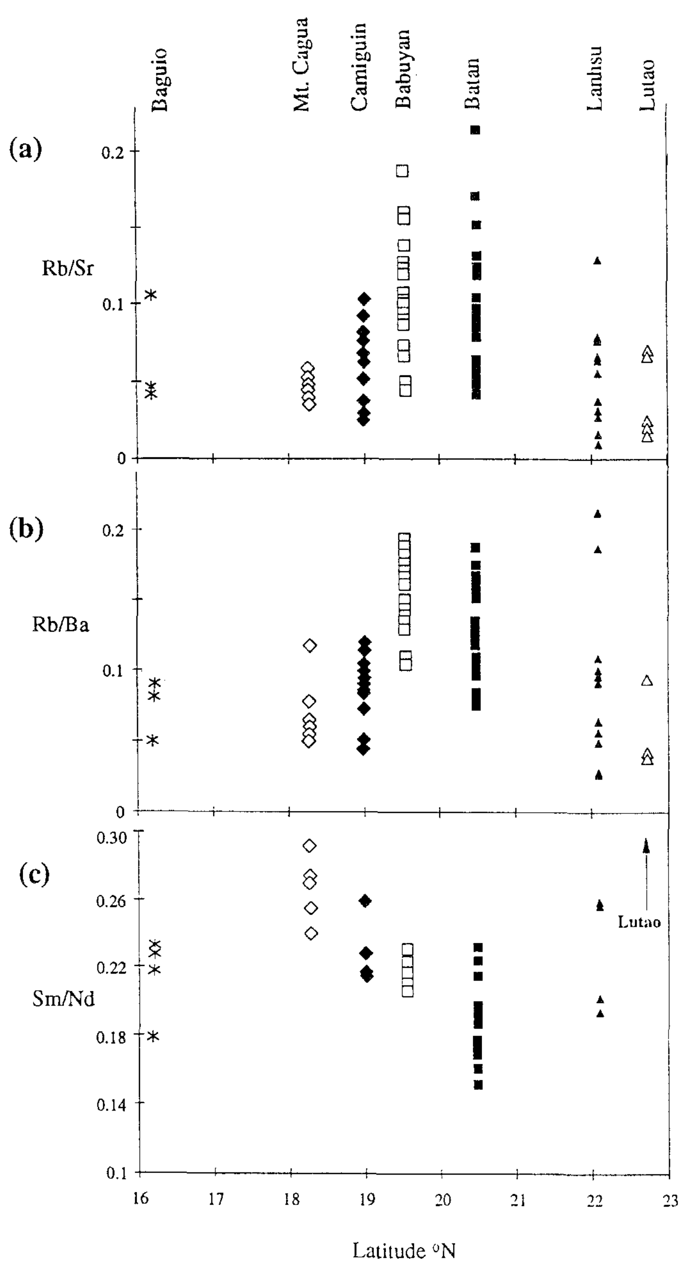

Fig. 3a–c. Latitudinal variations in **a** Rb/Sr; **b** Rb/Ba; **c** Sm/Nd ratios in young (< 3 Ma) volcanics from the N. Luzon arc. Data symbols as in Fig. 2

(0.70435–0.70545). The processes responsible for these isotopic variations, and for their displacement below the Nd-Sr mantle array are discussed further later.

Pb-isotopes

The N Luzon rocks have relatively low $^{206}Pb/^{204}Pb$ compared with other subduction-related suites, and they plot above the Northern Hemisphere reference line (NHRL) (Hart 1984). Low $^{206}Pb/^{204}Pb$, accompanied by relatively high $^{207}Pb/^{204}Pb$ and $^{208}Pb/^{204}Pb$ is a feature of the so-called "Dupal" isotope anomaly (Hart 1984), and these isotope characteristics were noted previously in both the Philippine island arcs 500–1000 km south of Luzon (Mukasa et al. 1987), and in MORB and OIB from the Philippine Sea (Hickey-Vargas 1991).

In detail, the Pb isotope data for the seven volcanic centres studied define a series of sub-parallel arrays (Fig. 5). Three aspects of the Pb isotope data are noteworthy. First, there is a systematic shift to higher $^{207}Pb/^{204}Pb$ and $^{208}Pb/^{204}Pb$ at a particular, $^{206}Pb/^{204}Pb$, along the arc from south to north. Thus,

Table 2. Selected major and trace element data for the N. Luzon volcanics

	SiO	MgO	TiO_2	K_2O	Ba	Rb	Sr	La	Nd	Sm	Yb	Zr	Hf	Ta	Ce
Batan															
B 46	53.2	7.45	0.73	2.30	547	87	1105	40.20	35.40	5.65	1.54		4.30		82.59
B 5	52.5	6.72	0.95	2.01	577	80	1206								
B 3M	53.6	3.58	0.95	2.27	626	107	648	38.50	38.40	6.46	1.82	196	4.80	0.63	73.7
B 10	54.0	3.63	0.97	2.11	600	99	880	48.81	44.19	7.79	1.84	250	5.48	0.73	106.9
B 1E	55.0	3.66	0.98	2.24	677	112	654	38.30	38.56	7.42	1.83	194	4.68	0.63	85.0
B 7	55.5	3.42	0.90	2.12	491	81	538	25.06	26.46	5.02	1.84				61.2
B 14	54.3	4.07	0.85	1.49	235	44	337	20.90		4.09	1.87	81	2.48	0.20	41.7
B 32	60.3	1.99	0.68	1.16	334	36	393	17.40		2.72	1.26	110	2.77	0.45	31.8
B 82	53.1	3.87	1.01	1.97	543	71	595	25.75	28.57	4.82	1.74	188	3.85	0.45	62.3
B 86	48.5	6.09	1.08	2.06	871	72	841	40.50		7.64	1.81	139	2.61	0.24	81.0
B 88	52.2	3.82	1.12	2.51	651	114	533	32.75	41.34	7.69	1.99	253	6.24	0.89	93.0
B 93	48.5	6.33	1.15	1.23	314	33	670	19.00	24.44	5.26	1.72	110	2.84	0.29	47.0
B 42	59.1	3.59	0.95	2.69	500	61	1170	26.68	30.49	6.33	1.26	169	3.91	0.37	55.7
B 80	51.9	7.90	0.81	1.11	272	21	497	13.10	17.20	3.70	1.46	85	2.25	0.23	27.6
Babuyan de Claro															
Bb 1	54.0	3.98	0.88	1.05	200	27	405	14.29	15.31	3.42	1.49	61	1.7	0.14	23.5
Bb 2	53.5	4.31	0.91	0.99	180	27	350	13.47	14.21	3.21	1.45	35	1.6	0.12	37.0
Bb 6	54.0	4.72	0.87	1.37	230	42	329	17.90		3.30	1.80	74	2.4	0.21	40.4
Bb 7	54.2	4.52	0.83	1.10	175	30	335	14.10		2.80	1.86	83	1.7	0.14	29.5
Bb 17	56.1	4.05	0.86	1.73	305	59	315	21.40		3.90	2.20	83	3.1	0.28	45.3
Bb 20	55.7	4.01	0.83	1.21	185	31	308	14.60		2.90	1.70	79	2.3	0.19	30.8
Bb 21	52.3	4.65	0.83	1.03	175	26	355	13.94	13.83	3.18	1.45	26	1.6	0.14	33.8
Bb 22	53.2	4.13	0.85	0.94	165	25	364	12.66	12.70	3.22	1.37	42	1.7	0.12	32.2
Bb 23	55.0	3.81	0.87	1.48	255	41	383	20.80		3.70	2.00	91	2.50	0.22	48.0
Bb 27	54.5	4.59	0.83	1.30	210	34	322	15.99		3.61	1.80	88	2.04	0.19	34.3
Bb 28	54.5	4.20	0.86	1.47	275	41	335	19.8		3.40	1.81	97	2.3	0.22	38.5
Bb 29	51.0			0.72	160	17	350								
Bb 3	54.0	3.35	0.92	1.46	260	43	348	23.88	21.33	4.71	1.86	89	2.49	0.22	50.2
Bb 31	54.0	4.20	0.94	1.32	250	37	360	18.27		3.67	1.72	54	2.03	0.18	33.5
Bb 36	56.0	3.59	0.88	1.65	230	40	333	21.20		3.88	1.90	88	2.44	0.24	41.0
Bb 38	53.8	4.25	0.94	1.41	230	40	333	21.20		3.80	1.90	88	2.44	0.24	43.2
Bb 39	51.3	5.21	0.81	0.74	140	15	342	10.00		2.30	1.55	38	1.40	0.11	20.0
Bb 40	56.7	3.33	0.88	1.75	280	52	326	22.90		4.10	2.30	95	2.90	0.27	46.0
Camiguin															
Cm 12	61.30	2.58	0.76	1.35	326	29	386	11.95	10.77	2.66	1.55	72	2.2	0.21	33.2
Cm 5	58.25	4.44	0.74	1.19	275	20	674	11.00		2.40	1.65	75	2.2	0.18	19.6
Cm 19	58.20	3.00	0.74	1.31	588	30	361	36.03		8.78	6.17	83	2.47	0.19	57.0
Cm 24	56.50	3.62	0.74	0.78	200	10	388	8.13	10.10	2.62	1.72				19.2
Cm 40	58.00	3.34	0.86	1.31	336	28	445		15.00	3.26	2.04				
Cm 43	58.25			1.21	283	12	322								
Cm 46	61.30			1.51	350	33	360								
Cm 48	59.00	2.56	0.80	1.61	290	34	328	13.60		3.10	2.34	109	3.0	0.23	29.6
Cm 50	56.00			1.18	210	24	353								
Cm 51	58.50	3.43	0.85	1.29	225	27	352	11.60		2.70	1.96	81	2.60	0.19	27.2
Cm 54	53.80	4.26	1.05	1.45	300	30	478	22.00		3.60	2.00	103	2.6	0.19	42.5
Cm 55	54.8			1.27	240	25	477								
Cm 33	60.50	2.57		1.35	335	26	414	12.74	11.13	2.64	1.45	73	2.16	0.21	26.8
Cm 35	61.50	2.62	0.72	1.39	357	26	445	11.06	10.24	2.37	1.46	60	2.17	0.23	23.1
Mt Cagua															
Ca 2	52.00	3.35	1.04	1.22	416	25	470	11.59	11.35	2.90	1.74				24.6
Ca 11	50.50	3.82	1.00	1.12	354	22	533	12.66	13.49	3.64	2.04	69	1.71	0.22	36.6
Ca 9	55.20	2.73	0.92	1.32	505	25	553	15.92	14.82	3.79	2.08				42.5
Ca 17	53.70	3.03	0.98	1.34	448	28	490	12.60	13.17	3.84	2.17				28.5
Ca 26	53.30	3.59	1.05	1.12	408	23	472	13.04	12.63	3.03	1.81				27.3
Lanhsu															
TW 30	52.30	4.28	0.60	0.95	277	26.5	349	16.30		2.87	1.87	102	2.44	0.20	33.5
TW 31	54.50	4.56	0.82	1.02	278	17.7	568	13.82	14.92	3.20	1.56	68	2.4	0.15	27.6
TW 32	53.10	6.42	0.73	0.58	138	13.3	354	7.83	9.49	2.46	1.71	74	1.6	0.10	17.1
Lutao															
TW 36	55.30	4.20	0.61	1.90	1135	61.0	2984	158.0	13.44	7.90	1.56	211	5.10	0.99	299.0
TW 40	56.20	4.17	0.54	1.99	1558	62.6	2896	165.0		8.10	2.50	274	5.30	0.98	285.0
TW 41	60.20	2.31	0.52	1.48	448	42.2	607	21.3		3.07	1.24	104	2.63	0.32	40.3
TW 42	59.60	2.85	0.51	1.35	502	47.5	710	23.4		2.67	1.19	127	9.98	0.41	44.7

Table 2 (continued)

	SiO	MgO	TiO_2	K_2O	Ba	Rb	Sr	La	Nd	Sm	Yb	Zr	Hf	Ta	Ce
Baguio															
47 A	48.50	4.19	1.29	1.07	227	19	506	13.1	18.80	4.00	2.40	107	2.68	0.255	26.2
38 A	51.50	3.79	1.41	2.02	386	47	346	21.3	29.00	6.30	4.30				45.4
PL 41	58.82	2.66	0.52	1.57	260	40	373	10.1	10.10	2.00	1.30	85	2.34	0.308	19.6
PL 72	63.58	1.69	0.44	1.62	278	23	533	22.3	18.50	2.70	1.30	97	2.57	0.543	31.9

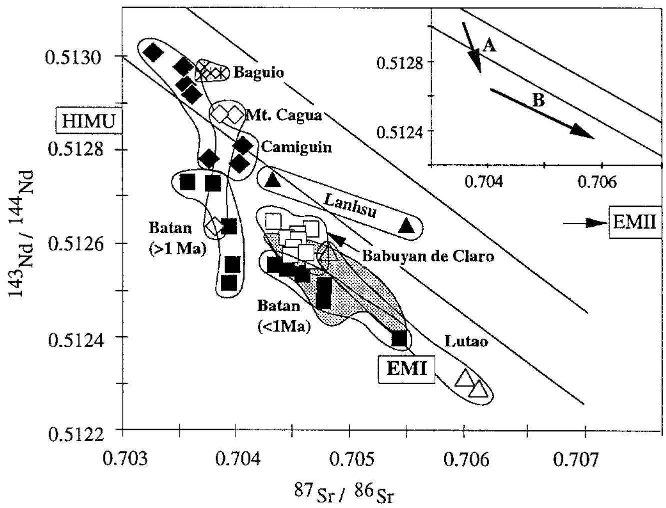

Fig. 4. $^{143}Nd/^{144}Nd$ versus $^{87}Sr/^{86}Sr$ diagram with data for the N Luzon volcanics. The "mantle array" (after White and Hofmann 1982) is shown for reference. The *stippled field* is for Batan xenoliths (Vidal et al. 1989). The HIMU and EM end-members are from Zindler and Hart 1986 and Hart et al. 1986. *Trends A* and *B* (*inset diagram*) reflect distinctive trace element ratio shifts discussed in the text (see Fig. 11)

the northern volcanoes, for example Batan, Lanhsu and Lutao have significantly higher $^{207}Pb/^{204}Pb$ and $^{208}Pb/^{204}Pb$, at a particular $^{206}Pb/^{204}Pb$ ratio, compared with those from Mt. Cagua in the south. Second, on a $^{208}Pb/^{204}Pb$ versus $^{206}Pb/^{204}Pb$ diagram the intra-island data arrays are sub-parallel to the NHRL, and so they trend towards an end-member with high $^{208}Pb/^{204}Pb$ at low $^{206}Pb/^{204}Pb$ such as, for example, Indian Ocean MORB (Mahoney et al. 1989: Hamelin et al. 1986) and Philippine Sea MORB (Hickey-Vargas, 1991), rather than towards the NHRL. Finally, with the exception of a single carbonate- rich sample (VM19-119, about 7 wt. % CaO), the Pb isotope data for the South China Sea piston-core lower-Pleistocene sediment samples have relatively radiogenic Pb isotope ratios, and define a field which is oblique to the data arrays for the Luzon arc volcanics in Fig. 5. In detail, these sediments also exhibit a systematic latitudinal shift in $^{208}Pb^*/^{206}Pb^*$, which reflects time integrated Th/U (Allègre et al. 1986), and it is argued later that the latitudinal Pb isotope variations in the volcanics reflect those in the subducted sediments. However, in such a mixing model the mantle wedge end-member has high

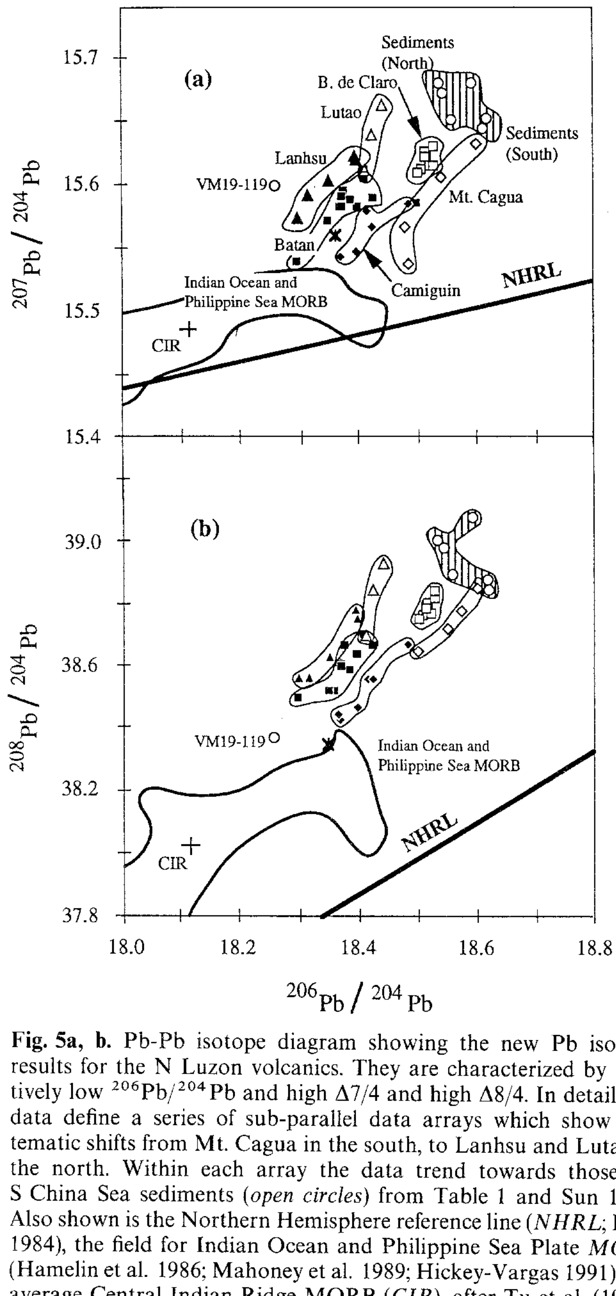

Fig. 5a, b. Pb-Pb isotope diagram showing the new Pb isotope results for the N Luzon volcanics. They are characterized by relatively low $^{206}Pb/^{204}Pb$ and high $\Delta 7/4$ and high $\Delta 8/4$. In detail, the data define a series of sub-parallel data arrays which show systematic shifts from Mt. Cagua in the south, to Lanhsu and Lutao in the north. Within each array the data trend towards those for S China Sea sediments (*open circles*) from Table 1 and Sun 1980. Also shown is the Northern Hemisphere reference line (*NHRL*; Hart 1984), the field for Indian Ocean and Philippine Sea Plate *MORB* (Hamelin et al. 1986; Mahoney et al. 1989; Hickey-Vargas 1991) and average Central Indian Ridge MORB (*CIR*), after Tu et al. (1992). *Data symbols* as in Fig. 2

$\Delta 8/4$ (vertical displacement above the NHRL, Hart 1984) similar to that of average Central Indian Ridge MORB (See CIR, Fig. 5).

Table 3. Isotope and selected trace element data for S. China Sea sediments

Sample	Latitude°N	$^{87}Sr/^{86}Sr$	$^{143}Nd/^{144}Nd$	$^{206}Pb/^{204}Pb$	$^{207}Pb/^{204}Pb$	$^{208}Pb/^{204}Pb$	$^{208}Pb^*/^{206}Pb^*$
VM19–119	17.250	0.70789	0.51262	18.257	15.600	38.365	0.993
RC17–156	19.617	0.71278	0.51222	18.542	15.673	38.980	1.029
RC17–159	20.317	0.71207	0.51219	18.558	15.651	38.896	1.018
RC14–90R	21.050	0.71499	0.51216	18.536	15.681	38.995	1.031

MORB and many OIB samples define arrays with negative and positive slopes on plots of $^{143}Nd/^{144}Nd$ versus $^{208}Pb^*/^{206}Pb^*$ and $^{87}Sr/^{86}Sr$ versus $^{208}Pb^*/^{206}Pb^*$ respectively (Fig. 6) reflecting the range in isotope ratios which typically occur in those portions of the mantle removed from zones of active subduction. The N Luzon rocks define steeper arrays, and so have lower $^{143}Nd/^{144}Nd$ and higher $^{87}Sr/^{86}Sr$ at a given $^{208}Pb^*/^{206}Pb^*$ value compared with the MORB-OIB array. Also shown in Fig. 6 are data for the S China Sea sediments (Table 3), and it is noteworthy that the some of the volcanics have $^{143}Nd/^{144}Nd$ ratios similar to those of the sediments whereas $^{87}Sr/^{86}Sr$ ratios are much lower in the volcanics.

Th isotopes

The application of short-lived nuclides in the ^{238}U decay chain to problems of magma genesis have been summarized in several recent papers (e.g. Condomines et al. 1988; Gill et al. 1990, Gill and Williams 1990). Disequilibria between ^{238}U and ^{230}Th can provide unique constraints on the timing and extent of Th/U fractionation during partial melting. In the case of mid-ocean ridge basalts for example, ($^{238}U/^{230}Th$) is typically < 1, indicating Th enrichments relative to U during partial melting. In contrast, most subduction-related lavas either plot close to the equiline on a ($^{230}Th/^{232}Th$) versus ($^{238}U/^{232}Th$) diagram, or are displaced to the right of the equiline with ($^{238}U/^{230}Th$) > 1. This may reflect preferential enrichment of U from the subducted slab and/or a different source mineralogy or melting regime compared with that of the MORB source (Gill and Williams 1990; McDermott and Hawkesworth 1991).

Many of the N Luzon lavas are either too old or too poorly dated to be suitable for whole-rock Th isotope measurements. However, samples from three Holocene lavas from Batan, and one from Babuyan de Claro were analyzed for ($^{230}Th/^{232}Th$) and ($^{238}U/^{232}Th$). ($^{230}Th/^{232}Th$) ratios are in the range 0.55–0.67, and so are lower than in the majority of destructive plate margin rocks (Fig. 7), indicating a source with unusually high Th/U. Moreover, the ($^{230}Th/^{232}Th$) ratios in the N Luzon volcanics are much lower than those in oceanic basalts (($^{230}Th/^{232}Th$) typically > 0.8, Condomines et al. 1988). Two samples (B3M, B10) plot within error of the equiline (Fig. 7), and the others (B1E and Bb 2) exhibits small amounts of excess U (about 5%) and so plot to the right of the equiline. Source Th/U, inferred from initial ($^{230}Th/^{232}Th$) varies from 4.54 in Babuyan de Claro to 5.5 in Batan.

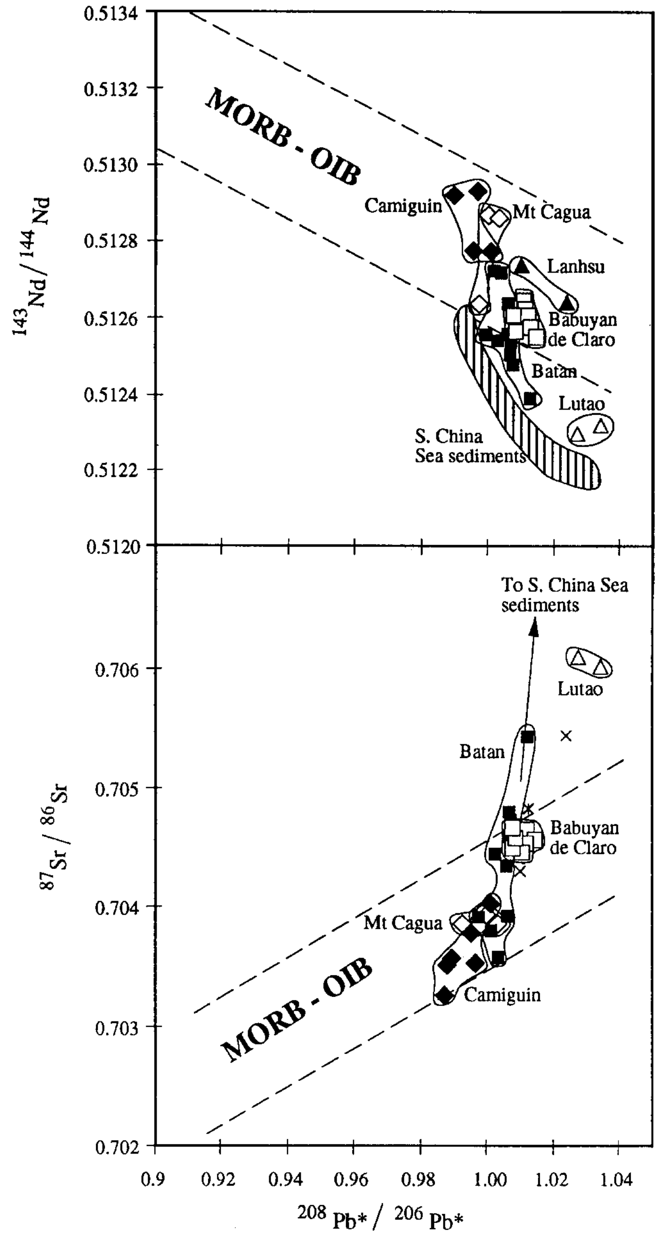

Fig. 6. MORB and many OIB define an array (*parallel dashed lines*) on plots of $^{143}Nd/^{144}Nd$ and $^{87}Sr/^{86}Sr$ versus $^{208}Pb^*/^{206}Pb^*$ (e.g. Rogers 1992). The N Luzon volcanics define arrays with a steeper slopes and extend to the field for S China Sea sediments (Table 1) on the $^{143}Nd/^{144}Nd$ versus $^{208}Pb^*/^{206}Pb^*$ diagram, but $^{87}Sr/^{86}Sr$ ratios are much lower than in the sediments (see text)

Terrigenous sediments are a low ($^{230}Th/^{232}Th$) reservoir by virtue of their high Th/U ratios, and in the S China Sea sediments Th/U varies from 4.8–7 (Table 3), which in secular equilibrium corresponds to a low

Table 3 (continued)

Sr	Nd	Rb	Sm	Ba	Th	U	TiO_2
371	15.7	54	3.5	527	5.6	2.4	0.66
228	23.3	108	4.2	530	9.9	2.0	0.77
258	23.3	108	4.5	523	9.2	1.9	0.74
177	28.0	117	5.4	507	10.5	1.5	0.80

($^{230}Th/^{232}Th$) ratio of 0.43 to 0.63. Thus, the low ($^{230}Th/^{232}Th$), combined with the absence of significant $^{230}Th/^{238}U$ disequilibria is consistent with the presence of subducted sediment in the source of the N Luzon lavas as discussed later.

Regional radiogenic isotope variations

Figure 8 summarizes the latitudinal variations in Nd, Sr and Pb isotopes. The $^{143}Nd/^{144}Nd$ decreases and while $^{87}Sr/^{86}Sr$ is more variable it tends to increase northwards (Fig. 8a, b). The data for the older (> 3.9 Ma) Lanhsu rocks are displaced to relatively high $^{143}Nd/^{144}Nd$ reflecting their shallow trend on the $^{143}Nd/^{144}Nd$ vs. $^{87}Sr/^{86}Sr$ diagram (Fig. 4). The latitudinal shift in Pb isotopes is best illustrated by the $^{208}Pb^*/^{206}Pb^*$ ratio, and this shows a broad northwards increase along the arc from Baguio to Lutao (Fig. 8c). The preliminary Th isotope data indicate a northward decrease in ($^{230}Th/^{232}Th$) from 0.67 in Babuyan de Claro to 0.55 in Batan, indicating that source Th/U ratios increased from about 4.54 in Mt. Cagua to > 5.5 in Batan. Since the Pb isotope ratios also indicate a northward increase in source Th/U (Fig. 8c), it may be further concluded that the north-south variations in source Th/U are relatively old (> 100 Ma). These, in turn, may reflect either the effect of subducted sediments containing an old crustal component or the presence of an old enriched mantle wedge (see discussion).

In summary, the isotope ratios of Sr, Nd and Pb in the N Luzon volcanics exhibit relatively smooth latitudinal variations (Fig. 8), so that time-integrated Rb/Sr and Th/U ratios increase from south to north, and Sm/Nd decreases. This contrasts with several of the measured trace element ratios (e.g. Rb/Sr, Sm/Nd, Rb/Ba) which tend towards maxima and minima near the centre of the arc (Fig. 3), and so the isotope and trace element ratios appear to behave coherently in the southern segment of the studied area from Mt. Cagua to Batan, and to be decoupled north of Batan (Figs. 3, 8). In detail, there is only a crude positive correlation between $^{143}Nd/^{144}Nd$ and Sm/Nd in the rocks from Mt. Cagua to Batan, but to generate the range in $^{143}Nd/^{144}Nd$ range from the observed range in Sm/Nd would take about 1 Ga.

The latitudinal isotope variations in the S China Sea sediments are also shown in Fig. 8. The $^{87}Sr/^{86}Sr$ in the sediments varies from 0.70701 to 0.71499 (Table 3), and it tends to increase northwards, probably reflecting the increased input of high $^{87}Sr/^{86}Sr$ continental detritus eroded from the Chinese continental shelf to the north. The $^{208}Pb^*/^{206}Pb^*$ also increases northwards in the sediment samples from about 0.991 in the south, to 1.031 in the north (Fig. 8). $^{143}Nd/^{144}Nd$ ratios vary from 0.51216 to 0.51262 and decrease northwards. Significantly, both the range and the absolute values of $^{87}Sr/^{86}Sr$ in the sediments are much greater than those the volcanics, and this contrasts with $^{143}Nd/^{144}Nd$ and $^{208}Pb^*/^{206}Pb^*$, both of which exhibit values and a range more similar to those in the sediments.

Thus, if subducted sediment is largely responsible for the observed isotope shifts in the volcanics, then some

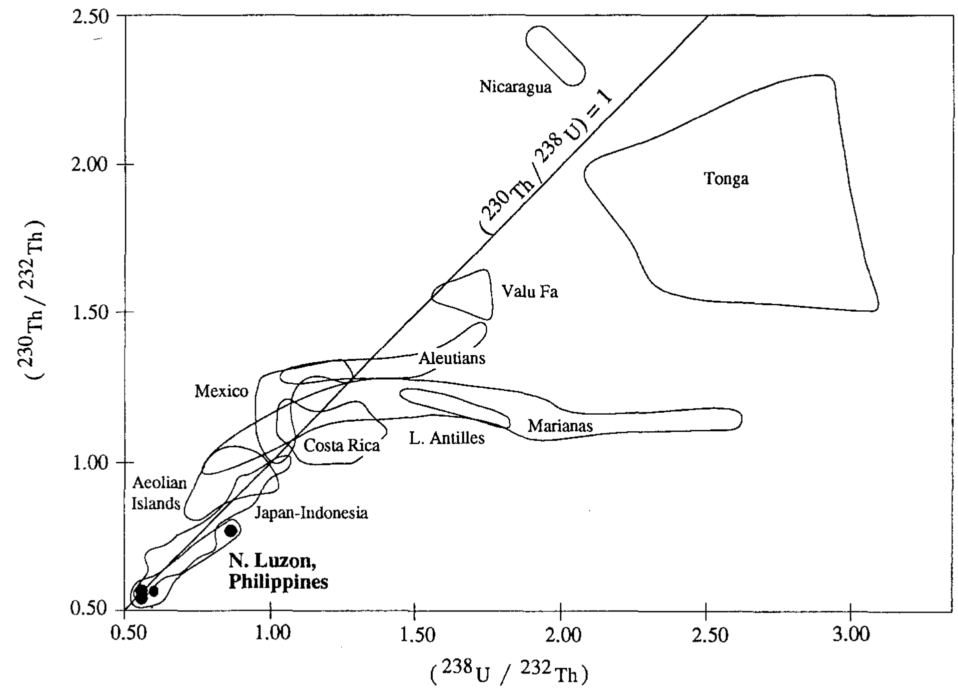

Fig. 7. ($^{230}Th/^{232}Th$)-($^{238}U/^{232}Th$) disequilibrium diagram showing the Th isotope ratios for selected N Luzon volcanics in relation to other subduction-related suites. (Data fields from McDermott and Hawkesworth 1991; Gill and Williams 1990 and references therein.)

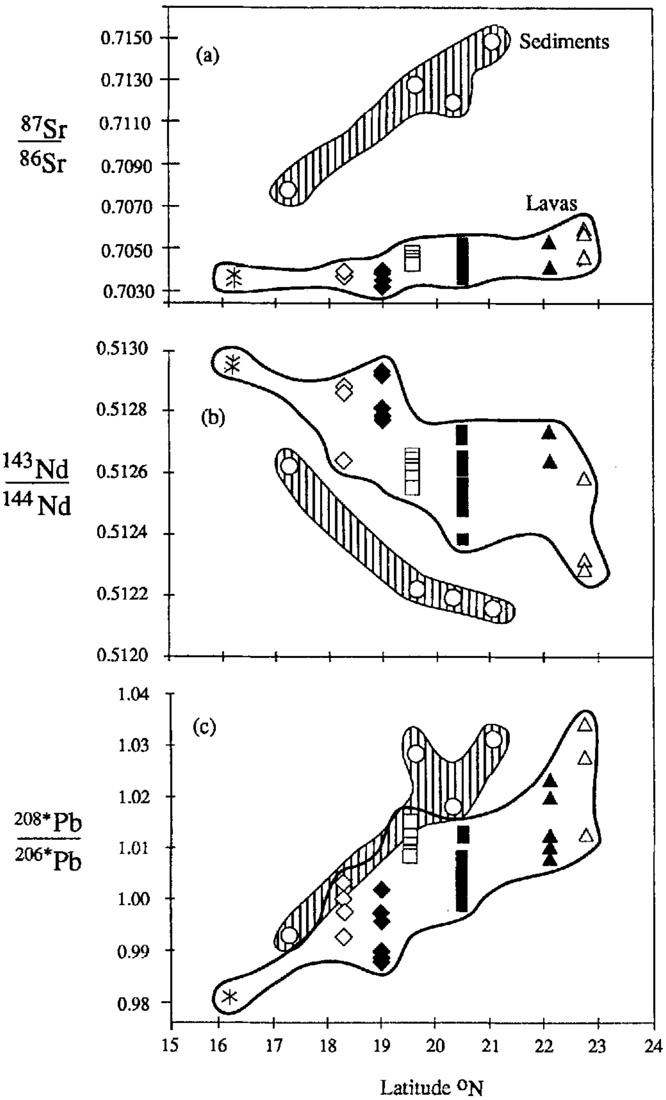

Fig. 8a–c. Latitudinal variations in $\mathbf{a}\,^{87}Sr/^{86}Sr$; $\mathbf{b}\,^{143}Nd/^{144}Nd$; $\mathbf{c}\,^{208}Pb^*/^{206}Pb^*$ in the N Luzon volcanics. *Symbols* for the lavas are as in Fig. 2. Also shown are latitudinal variations in $^{87}Sr/^{86}Sr$, $^{208}Pb^*/^{206}Pb^*$ and $^{143}Nd/^{144}Nd$ in the S China Sea sediments (*circles in lined data field*, Table 3). Note that the range in $^{87}Sr/^{86}Sr$ is much greater in the sediments compared with the volcanics

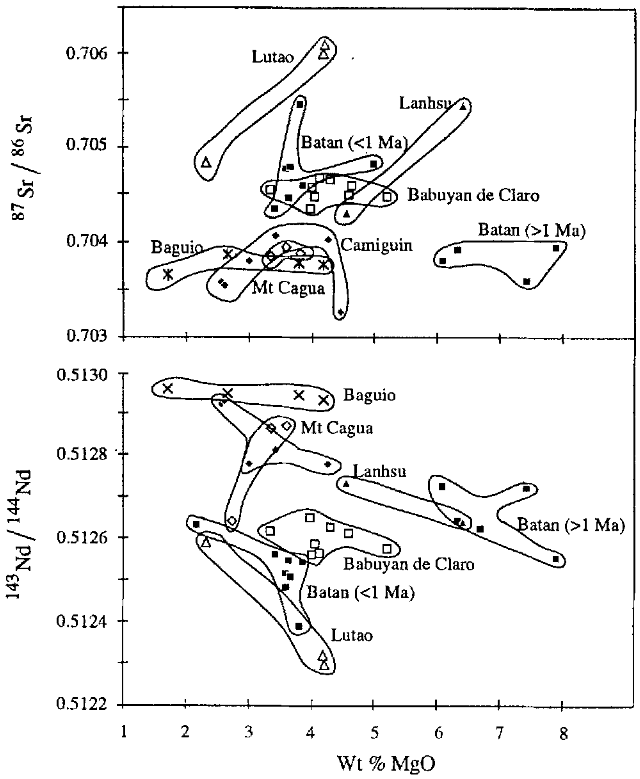

Fig. 9. $^{87}Sr/^{86}Sr$ and $^{143}Nd/^{144}Nd$ versus MgO in the N Luzon volcanics demonstrating that within each suite the most enriched isotope ratios (higher $^{87}Sr/^{86}Sr$ and lower $^{143}Nd/^{144}Nd$) tend to occur in the rocks with the higher MgO contents

explanation is required for the relatively small shifts in $^{87}Sr/^{86}Sr$. In principle, the smaller range in $^{87}Sr/^{86}Sr$ in the volcanics might reflect different Sr contents in the subducted sediment if they decreased northwards. There is some evidence that this occurs, with Sr contents decreasing by about a factor of two in the sediments from south to north (Table 3), but simple mixing calculations reveal that this decrease is not sufficient to compensate for the large northward increases in $^{87}Sr/^{86}Sr$ observed in the sediments. Thus, a binary mixing model between a mantle wedge end-member and subducted sediment cannot account for the observed variations in Sr isotope variations in the volcanics, although addition of $< 5\%$ of bulk sediment could account for the Nd and Pb isotope variations. Moreover, the trace element geochemistry of the volcanics requires a third component, namely a LIL element enriched slab-derived fluid (see discussion later and Fig. 11), and it is further argued that this component has high Sr/Nd, and that it partially buffers $^{87}Sr/^{86}Sr$ in the volcanics.

The role of crustal contamination

Several lines of evidence indicate that the enriched isotope signature of the N Luzon volcanics was not primarily due to crustal contamination processes. First, covariations between MgO and $^{143}Nd/^{144}Nd$ and $^{87}Sr/^{86}Sr$ show that it is the least differentiated, highest MgO rocks in each suite which tend to have the most enriched isotope ratios, and in particular the lowest $^{143}Nd/^{144}Nd$ (Fig. 9). We conclude that combined fractional crystallization and assimilation processes are unlikely to been primarily responsible for the enriched isotope signature of the N Luzon lavas. Further evidence for the lack of significant crustal contamination is provided by recent O isotope studies. Chen et al. (1990) and Fourcade et al., (in press) demonstrated that the N Luzon lavas have a very restricted range in $\delta^{18}O$ (5.97–7.14%), and in their comprehensive $\delta^{18}O$ study of fifty samples from along the N Luzon arc Fourcade et al. (in press) concluded that 'source contamination' was responsible for the radiogenic isotope variations, and that minor crustal contamination was detectable only in the south of the arc (at Baguio and Camiguin). Combined $\delta^{18}O$, Sr, Nd and Pb isotope data further indicate that where minor crustal contamination may have occurred in the south of the arc it resulted in only small shifts in radiogenic isotope ratios, for example, a shift from 0.70366 to 0.70388 in Baguio (in press). Thus, while crustal contamination may have been responsible for some of the range in $^{87}Sr/^{86}Sr$ and $^{143}Nd/^{144}Nd$ *within* the Baguio and Camiguin suites, it does not appear to have been responsible for the inter-suite latitudinal isotope shifts (Figs. 4, 5, 8, 11) which are the subject of this study.

Discussion

The results presented here have documented striking north-south variations in the isotope and trace element ratios of the post-3 Ma rocks of the N Luzon arc, and systematic isotopic shifts with latitude in sediments from the S China Sea. In the following section we combine the trace element and isotope data to address the following key questions. What are the processes responsible for the trace element characteristics of the North Luzon lavas, namely relatively high LIL element and LREE abundances, and low HFS elements? To what extent does the enriched isotopic signature reflect pre-existing trace element enriched mantle in the wedge rather than subducted sediment? Can trace element ratios be used to isolate the contributions from subducted sediment, hydrous fluids released from the slab, and the mantle wedge?

LIL element enrichment

In principle, the 'excess' LIL and LREE element contents in the N Luzon lavas could reflect either a contribution from the subducted slab, and/or elements scavenged from the overlying mantle wedge by slab-derived hydrous fluids, and so it is simply referred to as the 'subduction component'. For elements such as K, there is considerable controversy over whether it is derived primarily from the mantle wedge, or from recycled material in the subducted slab (Kay 1980; Hawkesworth and Ellam 1989). The N Luzon lavas show a five-fold variation in K_2O (about 0.50–2.60 wt. %) and, as in other high Ce/Yb subduction-related suites, there is a broad positive correlation between K_2O and Ce/Yb (Fig. 2b). Thus, if a slab-derived component is invoked to explain the range in K contents, it would appear that it contains significant quantities of LREEs, and so it will also affect $^{143}Nd/^{144}Nd$. A plot of K/Yb versus Ta/Yb has been used previously (Pearce 1983) to discriminate between the effects of intra-mantle melt-related trace element enrichment, and addition of a slab-derived fluid or 'subduction component'. The basis for this diagram is that a slab-derived fluid increases K/Yb, but Ta/Yb remains relatively unaffected; thus the shift to high K/Ta, relative to MORB and OIB, observed in many subduction-related lavas may be attributed to the effect of a slab-derived fluid. Moreover, the constancy of K/Ta in MORB and OIB (average K/Ta = 4545 and 4444, respectively, Sun and McDonough 1989) testifies to the similar incompatibility of these elements during mantle melting, and so it is argued that this element ratio should not be fractionated by partial melting, unless a Ta-rich phase is present in the residue. McCulloch and Gamble (1991) argued that HFS element anomalies in subduction-related lavas are caused not by HFS-rich residual phases, but by preferential enrichments of the LIL and LREE elements by slab-derived hydrous fluids, and the following discussion is based on the premise that variations in K/Ta and La/Ta reflect K and La enrichment via the slab-derived fluid and are not the product of variable degrees of partial melting.

Figure 10 illustrates the variations in K/Yb, La/Yb and Ta/Yb in the Philippine rocks, and emphasises their relatively high K/Ta and La/Ta ratios. Assuming that K/Ta and La/Ta ratios are not fractionated significantly by partial melting, then the range in K/Ta and La/Ta reflects either variations in the amount of added 'subduction component' (e.g. K and La) and/or pre-existing variations in the Ta contents of the mantle wedge. In practice both processes play a part, but Ta abundances which are thought to be unaffected by the added 'subduction component', vary by a factor of ten, whereas La

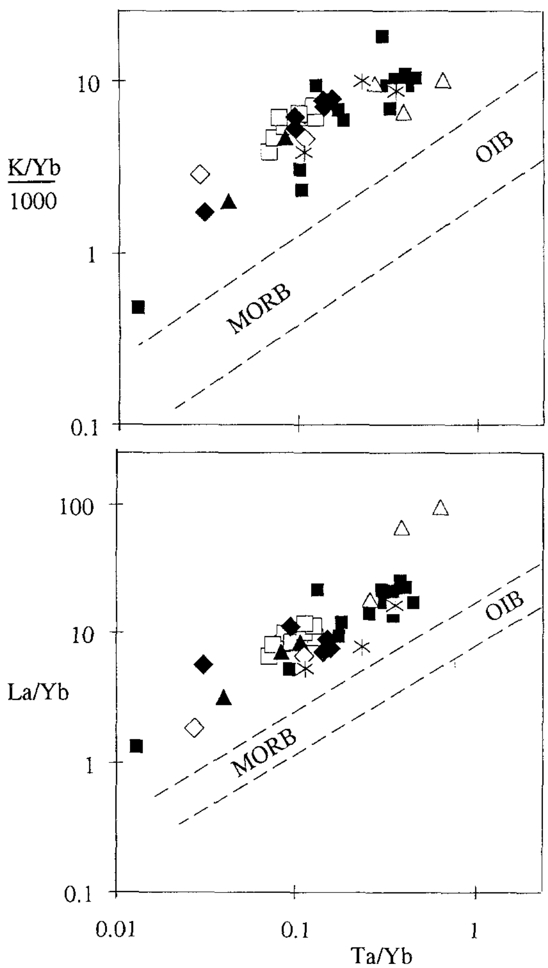

Fig. 10. K/Yb and La/Yb versus Ta/Yb for the N Luzon volcanics. Also shown are the MORB-OIB arrays which reflect intra-mantle partial melting processes (after Pearce 1983). The introduction of a subduction component is inferred to result in a vertical vector (K/Yb and La/Yb increase but Ta/Yb is relatively unaffected). Data symbols as in Fig. 2

and K concentrations vary by less than a factor of five, suggesting that pre-existing enrichments and depletions in the mantle wedge, and/or addition of Ta by bulk addition of subducted sediment (see later) is the dominant control on K/Ta and La/Ta ratios.

Figure 11 illustrates the variations in $^{143}Nd/^{144}Nd$ that accompany the shifts in trace element ratios. Yb contents vary only by a factor of two in the N Luzon rocks (Table 2), so that the large variations in Ta/Yb (Fig. 11a) largely reflect variations in Ta. However the variations in Ta/Yb are accompanied by systematic changes in radiogenic isotopes (e.g. $^{143}Nd/^{144}Nd$, Fig. 11a), and so they cannot simply reflect differences in Ta abundances caused by different degrees of partial melting at the time of magmatism in the N Luzon arc. The decrease in Ta/Yb in the south of the arc (trend A, Fig. 11) largely reflects variations in Ta abundance and this, in turn, might reflect pre-existing source depletion with the lowest Ta/Yb rocks near the centre of the arc at Camiguin. In the northern part of the arc (trend B, Fig. 11) increases in Ta, and so Ta/Yb, with decreasing $^{143}Nd/^{144}Nd$ are attributed to bulk addition of subducted sediment, or a melt thereof, rather than to segments of old enriched mantle in the wedge (see later).

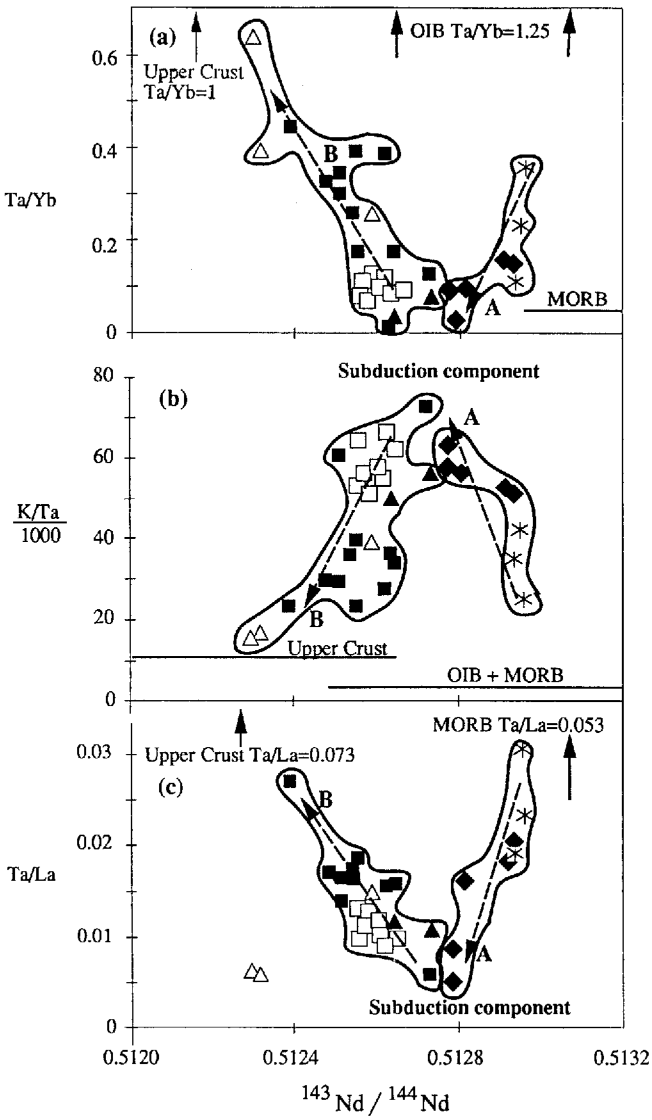

Fig. 11a–c. Variations in Ta/Yb, K/Ta and Ta/La with $^{143}Nd/^{144}Nd$ indicate that three end-members are required to explain the N Luzon arc data. *Trends A* and *B* coincide with isotope shifts shown in Fig. 4 (*inset*). Data symbols as in Fig. 2

Evidence for three end-members

The striking feature of the trace element ratio - $^{143}Nd/^{144}Nd$ arrays of Fig. 11 is that they all exhibit a sharp kink at $^{143}Nd/^{144}Nd$ = about 0.51275. This is part of the reason for the identification of two trends, A and B, on the Nd-Sr isotope diagram (Fig. 4), in that the rocks from Baguio and Camiguin tend to have the higher $^{143}Nd/^{144}Nd$ ratios and a restricted range in $^{87}Sr/^{86}Sr$, and they comprise trend A. Moreover, the presence of two trends in Figs. 4 and 11 reaffirms that at least three components are represented in the observed chemical variations. These are: (1) a high $^{143}Nd/^{144}Nd$, low LIL/HFS end-member best developed in Baguio, (2) a high LIL/HFS component which is best developed in the HFS depleted rocks on Camiguin and Babuyan de Claro, and (3) a low $^{143}Nd/^{144}Nd$ end-member seen in Lutao and in many of the Batan samples (Fig. 11).

Subducted sediment or enriched mantle?

A key question is the extent to which the northward shift to enriched isotope ratios reflects sediment subduction or pre-existing enrichments in the mantle wedge. The coupled latitudinal isotope variations in the arc volcanics and the S China Sea sediments strongly suggest that subducted sediment was implicated in the generation of the isotope shifts in the volcanics. We note, however, that similar ranges of Sr, Nd and Pb isotope ratios occur in portions of enriched mantle sampled by some ocean island basalts (Zindler and Hart 1986), and so other criteria are required to distinguish contributions from subducted sediment and pre-existing compositions in the mantle wedge. Unfortunately, many incompatible trace element ratios are similar in enriched mantle and terrigenous sediments, but a few trace element ratios can usefully distinguish between these reservoirs. Rb/Ba ratios, for example, are typically twice as high in terrigenous sediments as in OIB (Fig. 12). Moreover, Rb and Ba are highly incompatible trace elements, and the similarity of Rb/Ba ratios in average OIB and MORB (0.089 vs. 0.09, Sun and McDonough 1989), implies that they are not fractionated significantly by partial melting in the upper mantle, and so mantle heterogeneities developed by melt infiltration processes are not expected to have high Rb/Ba. With the exception of the Lutao samples, the low $^{143}Nd/^{144}Nd$ rocks tend to have high Rb/Ba ratios which are not readily explained by intra-mantle melt-related enrichment processes, but they are consistent with the bulk addition of < 5% subducted sediment.

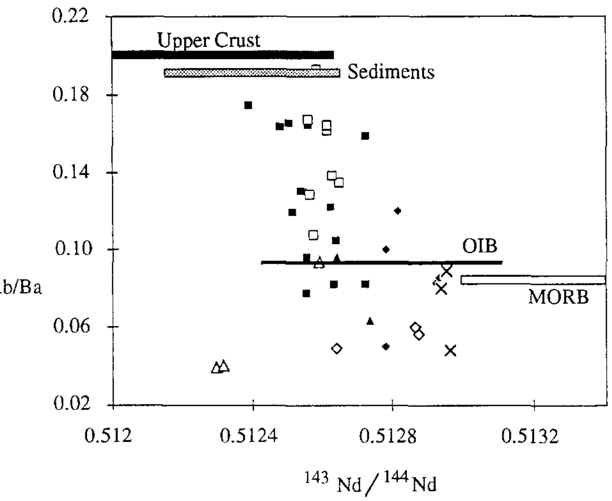

Fig. 12. Variations in Rb/Ba with $^{143}Nd/^{144}Nd$ in the N Luzon volcanics. Also shown are typical values for average upper crust (Taylor and McLennan 1985) the average values for the S China Sea sediments (Table 3). The high Rb/Ba ratios of the low $^{143}Nd/^{144}Nd$ rocks are interpreted as reflecting bulk addition of subducted sediment. Data symbols as in Fig. 2

The lavas yield relatively old depleted mantle Nd model ages in the range 0.14 to 1.2 Ga, and samples from Batan and Babuyan de Claro have the oldest Nd model ages (0.72–1.23 Ga) reflecting their unradiogenic Nd isotope ratios. As discussed previously, the mantle lithosphere in this region is unlikely to be older than the Tertiary according to recently published geodynamic reconstructions (Rangin et al. 1990), and so the mantle wedge is apparently too young to have generated the unradiogenic Nd isotope ratios by in situ radioactive decay. In the simplest model, the unradiogenic Nd isotope compositions therefore reflect a component introduced by the subduction process, and since this component appears to contain HFS elements (e.g. Ta, high Ta/Yb in Fig. 11) it is not the fluid-related 'subduction component' as previously defined. Rather, it is concluded that the end-member with the lowest $^{143}Nd/^{144}Nd$ is subducted sediment, and because the sediment was added in bulk it transferred HFS elements, including Ta into the mantle wedge. The $^{208}Pb^{*}/^{206}Pb^{*}$ also increases northwards in both the S China Sea sediments and the volcanics (Fig. 8), and so in the preferred model, the latitudinal variations in Pb isotopes in the volcanics largely reflect those in subducted sediment. Simple mixing calculations indicate that $< 5\%$ bulk subducted sediment added to a mantle wedge similar to that of the Central Indian Ridge (CIR, Fig. 5) is sufficient to generate the observed Pb-Pb arrays. Moreover, bulk mixing of about 3% subducted sediment can explain the low ($^{230}Th/^{232}Th$) ratios, and the lack of U-Th disequilibria in the Batan volcanics. The absence of significant U-Th disequilibria in the Batan samples requires that Th/U ratios were not fractionated when sediment addition occurred, and this is best explained by the introduction of bulk sediment. This interpretation implies that a large proportion ($> 50\%$) of the Pb, Nd and Th abundances were derived from subducted sediment. Sr isotopes, by contrast, appear to reflect a greater contribution from a slab-derived fluid. We note also that the new Pb isotope data reported here do not appear to be consistent with the contention of Chen et al. (1990) that an EMI component was involved in the genesis of the N Luzon lavas. The $^{206}Pb/^{204}Pb$ ratio of the EMI component is much lower (about 17.25) than those of the N Luzon lavas, and the simplest interpretation is that the low $^{206}Pb/^{204}Pb$ mantle wedge end-member had elevated $^{207}Pb/^{204}Pb$ and $^{208}Pb/^{204}Pb$, similar to that seen in Indian Ocean MORB (Mahoney et al. 1989) and MORB erupted on the Philippine Sea Plate (Hickey-Vargas 1992).

The 'subduction component'

High K/Ta and low Ta/La ratios are ascribed to the 'subduction component', but to what extent does the shift from Baguio to Camiguin (trend A, Fig. 11) reflect latitudinal variations in the *amount* of the subduction component, and/or pre-existing trace element variations in the mantle wedge. The Camiguin Island samples have significantly lower Ta contents than those from Baguio (Table 2), and so much of the shift in K/Ta and La/Ta reflects a more depleted mantle wedge beneath Camiguin Island. However, the striking observation is that the samples from Camiguin Island and Babuyan de Claro which have the lowest Ta/La and highest K/Ta ratios (Fig. 11) have similar, but relatively low $^{143}Nd/^{144}Nd$ ratios (about 0.51275). This suggests that the 'subduction component' contains Nd with a $^{143}Nd/^{144}Nd$ ratios of approximately 0.51275, and as it appears to have been responsible for trend A (Fig. 4) it contains Sr with an $^{87}Sr/^{86}Sr$ ratio of about 0.7040. In this arc, therefore, the addition of a subduction component, recognized on the basis of high LIL/HFS ratios, has resulted in a near vertical shift on the Nd-Sr isotope diagram. This contrasts sharply with the conclusions of several studies on other arc suites, in which the development of high LIL/HFSE ratios was associated with a sub-horizontal displacement to relatively high $^{87}Sr/^{86}Sr$ (De Paolo and Wasserburg 1977; Hawkesworth et al. 1977; Ellam and Hawkesworth 1989).

The consequences of adding the subduction component with $^{87}Sr/^{86}Sr = 0.7040$ and $^{143}Nd/^{144}Nd = 0.51275$ to a mantle wedge affected by subducted sediment are explored in Fig. 13. In practice the 'subduction component' represents an inflexion point where mixing curves change from being convex upwards to being concave upwards. Such a three component mixing model explains why many of the N Luzon lavas plot below the Nd-Sr mantle array, and accounts for the observed increase in K/Ta and La/Ta in those samples with $^{143}Nd/^{144}Nd$ ratio of about 0.5127. The relatively low $^{143}Nd/^{144}Nd$ ratio of the subduction component indicates that the slab-derived fluids, which are held to be responsible for the high LIL/HFS ratios, included contributions from subducted sediment as well as the meta-igneous rocks of the oceanic crust, and that they carried significant amounts of Nd. The $^{87}Sr/^{86}Sr$ ratio of the subduction component is less well constrained, but the Nd-Sr isotope covariations indicate that it was approximately 0.7040, which, in turn, implies either that the unaltered oceanic crust contributed

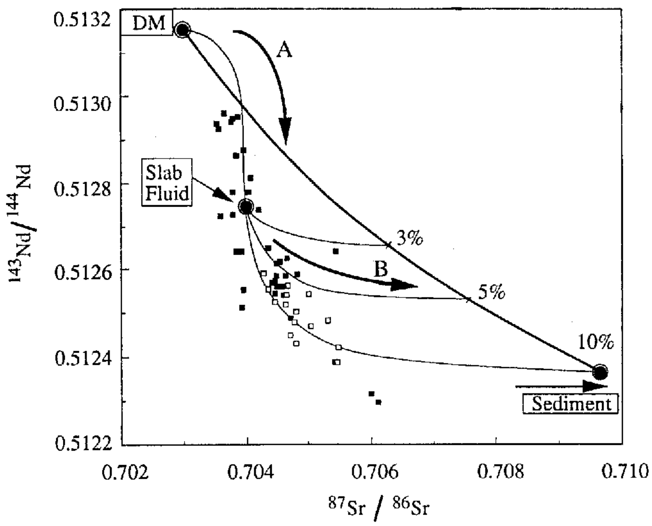

Fig. 13. Three component mixing model which accounts for the position of the N Luzon volcanics below the Nd-Sr mantle array, and the trace element ratio maxima and minima which occur at $^{143}Nd/^{144}Nd = 0.51275$ (Fig. 11). Mixing curve parameters are as follows: depleted mantle (*DM*) $^{87}Sr/^{86}Sr$ = 0.703, $^{143}Nd/^{144}Nd$ = 0.51315, Sr = 14 ppm, Nd = 0.8 ppm; *sediment* $^{87}Sr/^{86}Sr$ = 0.714, $^{143}Nd/^{144}Nd$ = 0.51215, Sr = 190ppm, Nd = 28ppm; *slab fluid* $^{87}Sr/^{86}Sr$ = 0.704, $^{143}Nd/^{144}Nd$ = 0.51275, Sr = 20ppm; Nd = 0.1ppm. Also shown are all the available Nd-Sr isotope data for the N Luzon volcanics (*solid symbols*) and xenoliths from Batan (*open symbols*). (Data from Table 1, Defant et al. 1990; Vidal et al. 1989)

a large fraction of the slab-derived Sr, or perhaps more likely, that Sr isotopes in the slab-derived fluid exchanged more efficiently with the mantle wedge than Nd isotopes.

Conclusions

1. The high Ce/Yb subduction-related magmas of the Philippines exhibit striking latitudinal variations in $^{87}Sr/^{86}Sr$, $^{143}Nd/^{144}Nd$ and $^{208}Pb^*/^{206}Pb^*$. Similar isotopic variations also occur in sediments westward of the Manila Trench, and it is argued that subducted terrigenous sediment was largely responsible for the Nd and Pb isotope variations in the volcanics. The available Nd and Pb isotope data are consistent with bulk mixing of $< 5\%$ subducted sediment.
2. The lavas define two trends on a Nd-Sr isotope diagram. Trend A is towards lower $^{143}Nd/^{144}Nd$ but with relatively little change in $^{87}Sr/^{86}Sr$, and is accompanied by increases in LIL/HFS ratios (increasing K/Ta, La/Ta) reflecting the influence of a slab-derived fluid. Trend B is also towards lower $^{143}Nd/^{144}Nd$, but is accompanied by a larger shift in $^{87}Sr/^{86}Sr$ and decreases in LIL/HFSE ratios. The latter trend reflects the influence of subducted sediment.
3. The $^{143}Nd/^{144}Nd$ ratio of the slab-derived fluid is approximately 0.51275 which is significantly lower than that inferred in other studies of subduction-related rocks (e.g. Ellam and Hawkesworth 1989), probably reflecting the antiquity of the Chinese continental crust from which the subducted terrigenous sediments were derived. This, in turn, implies that the slab-derived fluid transferred Nd from the subducted slab to the overlying mantle wedge.
4. The relatively low $^{87}Sr/^{86}Sr$ ratio ($\sim$ 0.7040) inferred for the slab-derived fluid implies either that the Sr was dominated by contributions from unaltered oceanic crust in the subducted slab, or perhaps more likely, that it reflects Sr isotope exchange between the slab fluid and the overlying mantle wedge.
5. Bulk mixing of subducted sediment can also account for the low ($^{230}Th/^{232}Th$) in the N Luzon lavas, and the lack of U-Th disequilibria in the Batan rocks. This in turn implies that a large proportion of the Th ($> 80\%$) is derived from subducted sediment.
6. Prior to sediment subduction, the mantle wedge had relatively low $^{206}Pb/^{204}Pb$ and high $\Delta 8/4$ and $\Delta 7/4$ similar to that of Indian Ocean and Philippine Sea Plate MORB. There is no compelling evidence for the involvement of an EMI component as previously suggested (Chen et al. 1991).

Acknowledgements. The comments by two referees are gratefully acknowledged. Additional reviews by Fred Hochstaedter and David Peate also improved earlier versions of the manuscript. Peter van Calsteren, Mabs Johnson and David Wright are thanked for their help in the radiogenic isotope laboratory. Radiogenic Isotope facilities at the Open University are supported by the NERC. The L-DGO Deep Sea Sample Repository (supported by NSF Grant OCE 88-00001 and the Office of Naval Research through Grant N00014-87-K-0204) is gratefully acknowledged for allowing access to the S China Sea sediment samples.

References

Allègre CJ, Dupré B, Lewin E (1986) Thorium/uranium ratio of the Earth. Chem Geol 56:219–227
Arculus RJ (1981) Island arc magmatism in relation to the evolution of the crust and mantle. Tectonophysics 7:113–133
Bellon H, Richard M, Jacques D, Maleterre P, Maury R, Stephan JF (1988) Geology and isotopic chronology of the Luzon magmatic arc. Int Symp Geodyn Evol East Eur Margin (Paris) (Abstr)
Catanzaro EJ (1967) Absolute isotopic abundance ratios of three common lead reference samples. Earth Planet Sci Lett 3:343–346
Chen CH, Shieh YN, Lee T, Chen CH, Mertzman SA (1990) Nd-Sr-O isotopic evidence for source contamination and an unusual mantle component under Luzon arc. Geochim Cosmochim Acta 54:2473–2483
Condomines M, Hemond Ch, Allègre CJ (1988) U-Th-Ra radioactive disequilibria and magmatic processes. Earth Planet Sci Lett 90:243–262
Defant MJ, Jacques D, Maury RC, de Boer JZ, Joron JL (1989) Geochemistry of the Luzon arc, Philippines. Geol Soc Am Bull 101:663–672
Defant MJ, Maury RC, Joron JL, Feigenson MD, Letterrier J, Bellon H, Jacques D, Richard M (1990) The geochemistry and tectonic setting of the northern section of the Luzon arc (the Philippines and Taiwan). Tectonophysics 183:187–205
De Paolo DJ, Wasserburg GJ (1977) The sources of island arcs as indicated by Nd and Sr isotopic studies. Geophys Res Lett 4:465–468
Ellam RM, Hawkesworth CJ (1988) Elemental and isotope variations in subduction related basalts: evidence for a three component model. Contrib Mineral Petrol 98:72–80
Fourcade S, Maury RC, Defant MJ, McDermott F (1993) ^{18}O isotope evidence for a crustal component in northern Luzon arc

lavas and ultramafic xenoliths: mantle source versus arc crust contamination. Earth Planet Sci Lett (in press)
Gill JB (1984) Sr-Pb-Nd isotopic evidence that both MORB and OIB sources contribute to oceanic island arc magmas in Fiji. Earth Planet Sci Lett 68:443–458
Gill JB, Williams RW (1990) Th isotopes and U-series studies of subduction-related volcanic rocks. Geochim Cosmochim Acta 54:1427–1442
Gill JB, Pyle D, Williams RW (1990) Igneous rocks. In: Ivanovich M, Harmon RS (eds), Uranium series disequilibrium, 2nd edn. Oxford University Press, Oxford, UK
Green TH (1980) Island-arc and continent-building magmatism. A review of petrogenetic models based on experimental petrology and geochemistry. Tectonophysics 63:367–385
Hamelin B, Dupré B, Allègre CJ (1986) Pb-Sr-Nd isotopic data of Indian Ocean Ridges: new evidence of large scale mapping of mantle heterogeneities. Earth Planet Sci Lett 76:288–298
Hart SR (1984) A large-scale isotope anomaly in the Southern Hemisphere mantle. Nature 309:753–757
Hart SR, Gerlach DC, White WM (1986) A possible new Sr-Nd-Pb mantle array and consequences for mantle mixing. Geochim Cosmochim Acta 50:1551–1557
Hayes DE, Lewis SD (1984) A geophysical study of the Manila Trench, Luzon, Philippines 1. Crustal structure, gravity and regional tectonic evolution. J Geophys Res 89:9171–9195
Hawkesworth CJ, Ellam RM (1989) Chemical fluxes and wedge replacement rates along Recent destructive plate margins. Geology 17:46–49
Hawkesworth CJ, O'Nions RK, Pankhurst RJ, Hamilton PJ, Evenson NM (1977) A geochemical study of island-arc and back-arc tholeiites from the Scotia Sea. Earth Planet Sci Lett 36:253–262
Hawkesworth CJ, O'Nions RK, Arculus RJ (1979) Nd and Sr isotope geochemistry of island arc volcanics, Grenada, Lesser Antilles. Earth Planet Sci Lett 45:237–248
Hawkesworth CJ, Hergt JM, Ellam RM, McDermott F (1991) Element fluxes associated with subduction related magmatism. Philos Trans R Soc London, 335 A:393–405
Hickey-Vargas R (1991) Isotope characteristics of submarine lavas from the Philippine Sea: implications for the origin of arc and basin magmas of the Philippine tectonic plate. Earth Planet Sci Lett 107:290–304
Jacques D (1987) Géologie et pétrographie de L'Archipel Babuyan et des Monts Tabungon et Cagua, Nord Luzon, Philippines : implications magmatologiques et géodynamiques: Thèse Doct Univ Jersité Bretagne Occidentale
Kay RW (1980) Volcanic arc magmas : implications of a melting-mixing model for element recycling in the crust-upper mantle system. J Geol 88:497–522
Kay RW, Sun SS, Lee-Hu CN (1978) Pb and Sr isotopes in volcanic rocks from the Aleutian Islands and Pribilof Islands, Alaska. Geochim Cosmochim Acta 42:263–272
Knittel U, Defant MJ, Raczek I (1988) Recent enrichment in the source region of arc magmas from Luzon island, Philippines: Sr and Nd isotopic evidence. Geology 16:73–76
Lan CY, Chen JJ, Lee T (1986) Rb-Sr isotopic study of andesites from Lu-Tao, Lan-Hsu and Hsiao-Lan-Lsu : eruption ages and isotopic heterogeneity. Bull Inst Earth Sci Acad Sin 6:211–226
Le Roux LE, Glendenin LE (1963) Half-life of ^{232}Th. Proc Natl Meet on Nuclear Energy, Pretoria South Africa, pp 83–94
Mahoney JJ, Natland JH, White WM, Poreda R, Bloomer SH, Fisher RL, Baxter AN (1989) Isotopic and geochemical provinces of the Western Indian Ocean spreading centers. J Geophys Res 94:4033–4052
Meadows JW, Armani RJ, Callis EL, Essling AM (1980) Half-life of ^{230}Th. Phys Rev C22:750–754
McCulloch MT, Gamble JA (1991) Geochemical and geodynamical constraints on subduction zone magmatism. Earth Planet Sci Lett 102:358–374
McDermott F, Hawkesworth CJ (1991) Th, Pb and Sr isotope variations in young island arc volcanics and oceanic sediments. Earth Planet Sci Lett 104:1–15
McDermott F, Elliott TR, van Calsteren P, Hawkesworth CJ (1992) Measurement of ^{230}Th/^{232}Th ratios by thermal ionisation mass-spectrometry. Isotope Geosci (in press)
Morris JD, Hart SR (1983) Isotopic and incompatible trace element constraints on the genesis of island arc volcanics from Cold Bay and Amak Island, Aleutians and implications for mantle structure. Geochim Cosmochim Acta 47:2015–2030
Mukasa SB, McCabe R, Gill JB (1987) Pb isotopic compositions of volcanic rocks in the west and east Philippine island arcs : presence of the Dupal isotopic anomaly. Earth Planet Sci Lett 84:153–164
Pearce JA (1983) Role of the sub-continental lithosphere in magma genesis at active continental margins. In : Hawkesworth CJ, Norry MJ (eds) Continental basalts and mantle xenoliths. Shiva, Nantwich, UK pp 230–249
Peccerillo A, Taylor SR (1976) Geochemistry of Eocene calc-alkaline volcanic rocks from the Kastomanu area, Northern Turkey. Contrib Mineral Petrol 58:63–81
Rangin C and the Tethys Pacific working group (1990) The quest for Tethys in the Western Pacific: 8 palaeogeodynamic maps for Cenozoic time. Bull Soc Geol Fr (8), VI, 907–913
Richard M, Maury RC, Bellon H, Stephan JF, Boirat JM, Calderon
A (1986) Geology of Mt, Irayo volcano and Batan Island, northern Philippines. Philipp Bull Volcanol : 1–27
Rogers NW (1992) Potassic magmatism as a key to trace-element enrichment processes in the upper mantle. J Volcanol Geotherm Res 50:85–99
Saunders AD, Tarney J, Weaver SD (1980) Transverse geochemical variations across the Antarctic Peninsula: implications for the genesis of calc-alkaline magmas. Earth Planet Sci Lett 46:344–360
Sun SS, (1980) Lead isotopic study of young volcanic rocks from mid-ocean ridges, ocean islands and island arcs. Philos Trans R Soc London 297 A:409–445
Sun SS, McDonough WF (1989) Chemical and isotopic systematics of oceanic basalts: implications for mantle composition and process. In: Saunders AD, Norry MJ (eds) Magmatism in ocean basins. Geol Soc Spec Publ 42:pp 313–345
Tatsumi Y, Hamilton DL, Nesbitt RW (1986) Chemical characteristics of fluid phase released from a subducted lithosphere and origin of arc magmas : evidence from high-pressure experiments and natural rocks. J Volcanol Geotherm Res 29:293–309
Taylor B, Hayes DE (1983) Origin and history of the South China basin. In: Hayes D (ed) The tectonic and geologic evolution of southeast Asian seas and islands, 2. Am Geophys Union Monogr 27:23–56
Taylor SR, McLennan SM (1985) The continental crust: its composition and evolution. Blackwell, Oxford, UK
Tu K, Flower MFJ, Carlson RW, Xie G, Chen CY, Zhang M (1992) Magmatism in the South China Basin 1. Isotopic and trace element evidence for an endogenous Dupal mantle component. Chem Geol 97:47–63
Vidal P, Dupuy C, Maury RC, Richard M (1989) Mantle metasomatism above subduction zones : trace and radiogenic isotopes in xenoliths from Batan Island, Philippines. Geology 17, 1115–1118
White WM, Hoffman AW (1982) Sr and Nd isotope geochemistry of oceanic basalts and mantle evolution. Nature 296:821–825
Zindler A, Hart S (1986) Chemical geodynamics. A Rev Earth Planet Sci 14:493–571

Editorial responsibility: J.Hoefs